ORIGINAL ARTICLE

Nr 2022;12 (2):130-143

Fascia Healing after Induced Tibialis Anterior Muscle Strain: an Experimental Study in Wistar Rats

N. Abu Elwafa[1], T. Mohammad[1], H. Wageh[1], M. M. Elias[1], M. Nabhan[1], N. Salah Hassan[2], A. Rehan Youssef[1,3]

[1] *Department of Physical Therapy for Musculoskeletal Disorders and Surgery, Faculty of Physical Therapy, Cairo University, Giza, Egypt*

[2] *Department of Pathology, National Research Center, Giza, Egypt*

[3] *Department of Physical Therapy for Musculoskeletal Disorders and Surgery, Faculty of Physical Therapy, Ahram Canadian University, Giza, Egypt*

CORRESPONDING AUTHOR:
Aliaa Rehan Youssef
Physical Therapy for Musculoskeletal Disorders and Surgery
Cairo University and Ahram Canadian University
24 Mohammed Koraim Street
Nasr City, Cairo, Egypt 11765
E-mail: aliaa.rehan@gmail.com; aliaa.rihan@pt.cu.edu.eg

DOI:
10.32098/mltj.02.2022.06

LEVEL OF EVIDENCE: 3B

SUMMARY

Background. Recurrence following muscle strain is a serious problem encountered in sports. Muscle and fascia are mechanically integrated in transmitting muscular force. Fascial injury has been associated with muscle strain which may explain its potential contribution to impaired muscle recovery. This study aimed at describing structural changes of fascia and muscle as well as limb function recovery during the various healing stages following strain injury in rodents.

Methods. Thirty-two adult male Wistar rats were randomly and equally divided into four groups: normal control and three muscle strain injury groups. Tibialis Anterior muscle was strained in the three injured groups then all rats were allowed free cage mobility until euthanasia after 2 days (acute group), 9 days (subacute group), or 21 days (chronic and normal groups). The sciatic function index was used to assess functional recovery while histopathology scoring and histomorphometry quantified tissue healing.

Results. Cellularity significantly increased in muscle and fascia tissues only in the acute stage ($p < 0.05$). Collagen degeneration was significant in the acute and subacute stages in muscle ($p < 0.05$), whereas fascia showed significant degeneration only at the subacute stage ($p < 0.05$). Fascia thickness significantly increased in all examined stages ($p < 0.05$), while muscle fibers width and interstitial dilatation increased only in the acute and subacute stages ($p < 0.05$). Muscle fibrosis was significant in the subacute and chronic stages ($p < 0.05$). Function was not significantly different between all groups at all examined stages ($p > 0.05$).

Conclusions. Strain injury involves all fascia and muscle structures. Healing of all structures occurs spontaneously by the chronic stage, except for fascia thickness and muscle fibrosis. Future studies are recommended to investigate whether incorporating fascia as a therapeutic goal would decrease muscle injury recurrence.

KEY WORDS

Connective tissue; fascia; histopathology; muscle strain; sciatic function index.

BACKGROUND

Fascia is an elastic and contractile connective tissue (CT) that integrates the musculoskeletal system anatomically and mechanically (1). Muscles have various forms of fascial CT, including endomysium, perimysium, epimysium and deep fascia (2). There are anatomic and mechanical linkages between muscle and fascia that allow muscle forces to be transmitted serially and longitudinally so that the whole body is interconnected (3). Muscle strain may occur secondary to eccentric overload (active) or excessive overstretch when muscles are not contracting (passive), with active eccentric strain being the most common (4). Active strain injury occurs due to inadequate compressive strength while the

passive strain occurs due to inability of the tissue to counter the applied force (5). In strain injury, isolated muscular lesion is rare whereas injury that involves other muscular CT is more commonly reported. Strain may occur at various sites, such as at the intramuscular, myofascial, myofascial/perifascial or musculotendinous regions (6). Although the muscle structural, functional, and mechanical changes after strain injury have been studied in various animal models including rats and rabbits (7, 8) and in humans (9), yet less attention has been paid to study fascial changes associated with strain injury. A couple of studies assessed fascial injury accompanying strain in humans using imaging techniques such as Magnetic Resonance Imaging (MRI) and Ultrasound (US) (10, 11), however, to authors' knowledge, the structural changes in fascia over the various healing stages have never been described systematically. Therefore, the purpose of this study was to describe the structural changes of Tibialis Anterior (TA) muscle and its neighboring crural fascia as well as functional lower limb recovery after induced tendon-stretch strain injury in Wistar rats. Understanding fascial changes associated with strain injury may direct clinicians' attention to consider fascia as an impaired structure during muscle strain rehabilitation in order to minimize recurrence.

MATERIALS AND METHODS

Experimental design

This is an observational longitudinal study. Thirty-two adult (7-9 weeks) male healthy Wistar rats weighting between 203-282 g (mean ± SD: 234 ± 22), were obtained from and housed at the animal facility of the Faculty of Medicine, Cairo University, Egypt. All animals housing, care and experimental procedures were approved by the Institutional Animal Care and Use Committee (IACUC) of Cairo University, Egypt (approval number: CU/111/F/31/18). This study followed strictly the ARRIVE statement for reporting experimental results in animal models.

Procedures

A sample size of eight animals per group was selected based on previous recommendations for studies investigating histomorphology and histomorphometry in animal models when no previous relevant data are available to calculate the needed sample (12). Animals were allocated randomly and equally into four groups using the Excel software random generation function as follows: 1) normal control, which served as a reference standard for normal tissue histological appearance and function; 2) acute injury, that was euthanized 48 hrs after injury in order to study changes associated with the inflammator stage (7); 3) subacute injury, that was euthanized on the 9th day after injury in order to investigate the regenerative stage where tissue regeneration and scar tissue maturation take place (7, 13); and 4) chronic injury, that was euthanized on the 21st day after injury in order to investigate changes during the remodeling phase of healing, where scar tissue is fully mature and muscle regeneration is almost complete (7, 13).

TA strain was induced in all injured groups using a valid non-invasive tendon-stretching model (14). Briefl , rats were weighted and anesthetized using intraperitoneal injection of ketamine/xylazine (100 and 20 mg/kg, respectively). Animals were then positioned in a custom-made wooden frame (20 × 12.5 × 7.5 cm^3) with the right hind limb positioned and strapped to a footplate, starting with the ankle dorsiflexed to 90° and the knee kept in extension. TA was strained by plantar flexing the ankle using an external weight corresponding to 150% of the animal's body weight. This weight was attached gradually to a hook fastened to the exterior of the footplate (**figure 1S**). A weight with an increment of 25% of body weight was added every one minute until the complete weight was hanged. The full weight was maintained for 20 min, and the whole procedure was repeated twice, with 3 min rest interval in between. All procedures were standardized during the whole experiment.

Animals were housed in standard cages (4 animals/cage), kept under controlled temperature and humidity and exposed to a balanced 12-hour on/off light cycle. All rats were allowed free access to water (*ad libitum*) and were fed standard commercial rodent chow diet. Further, they were allowed free cage mobility until their euthanasia. Prior to euthanasia, the Sciatic Function Index (SFI) was measured *in vivo* to assess lower extremity kinematics. SFI is a valid and reliable assessment tool that scores between 0% (± 11; normal) and - 100% (complete loss of function) (15). Briefly, animal's paws were stained with ink, then they were motivated to walk across a walkway that was lined with squared paper sheets. Before actual data collection, rats were allowed a few conditioning trials. All trials were recorded simultaneously using a video camera to guide footprint selection based on their quality.

Two independent investigators selected the most representative walking footprints, then all sheets were coded and concealed using randomly generated numbers from excel software by a third researcher who was not involved in SFI measurements. Concealed prints were scanned, saved as images on a personal computer, then they were measured using the Kinovea software, which is an open access application for gait analysis (version 0.8.15, https://www.kinovea.org) (16). Two independent blinded assessors measured the following parameters on each image and an average was calculated: normal print length (NPL), experimental print length (EPL), experimental toe spread (ETS), normal toe spread (NTS), experimental intermediary toe spread (EIT)

and normal intermediary toe spread (NIT). The SFI score was calculated using the following equation (17):

SFI = - 38.3 × [(EPL - NPL)/(NPL)] + 109.5 × [(ETS-NTS)/(NTS)] + 13.3 × [(EIT-NIT)/(NIT)] - 8.8

Immediately following euthanasia using cervical dislocation, the skin and superficial fascia of the strained hind limbs were cut open. An incision was made on the lateral border of crural fascia that covers the TA in order to free the muscle and its overlying part of the deep fascia from the surroundings. Muscle and fascia were harvested and fixe in 10% neutral-buffered formalin for 48 hrs. Then, they were dehydrated in a series of graded alcohol and Xylene and prepared for histological processing following standard protocols. Tissues were embedded in paraffin and stored until they were cut into longitudinal 3µ thickness sections with a sampling rate of 1:6. Sections were then mounted on glass slides and stained using Hematoxylin and Eosin (H & E) and Masson trichome stains. Slides labels were coded, concealed and they were kept unbroken until all slides scoring was completed, verified, and entered into spreadsheets for further statistical analysis. The area of myotendinous junction (MTJ) with its overlying muscular and fascial (deep fascia and muscular CT) tissues which are the main site of strain lesion (13) were chosen as the area of interest. A single blinded trained assessor evaluated all slides under light microscopy for histomorphological assessment. Images were captured using a microscopy mounted camera (q500iw, Olympus, Japan) before histomorphometry was assessed using the Image J software (https://imagej.en.softonic.com) under magnifications ranging from 100x to 400x. Slides were assessed twice with a one-week interval in between.

The primary outcome for this study was fascia histomorphometry including fascia thickness, collagen area (%) and density, fibrocytes area (%), as well as fibrocytes nucleus perimeter and inflammatory area (%). Measures were done employing methods adopted from scoring systems of fasciae and other CT (18, 19). All these measures were conducted on H & E stained slides, except for collagen area (%) and density that were assessed using Masson trichome stained slides. Briefl , fascia thickness (µm) was measured to reflect on the overall change in fascia structure, a parameter reflec - ing tissue flexibilit , stiffness and fluid dynamics. Thickness was measured at 100x magnification using the straight-line tool function of image J for three times at different sites: two measures were taken at fascia periphery and one at the middle (18). The average of the three measures was calculated and used for further statistical analysis.

Collagen constitutes a key component in fascia that commonly shows signs of degeneration or increased scarring following strain injury and reflects the tissue tensile strength (7, 13). Collagen was quantified by measuring collagen area (%) and integrated density (IntDen). The area (%) represents the number of pixels or "%" of the specified color in the image while the IntDen is the pixel intensity or the amount of collagen stain present. The increase in both parameters indicate increased collagen synthesis and the reverse is true. Both parameters were measured in five fields at 100x by using the split function and green color thresholding in the image J software (18).

Fibrocytes and inflammatory cells increased number and size may reflect the intensity of inflammatory reaction induced by the strain injury. These cells were quantified in six images at 400x magnification using red components thresholding employing the split function of image J, which analyzes the area percentage of cells and the perimeter of nuclei (µm) (19).

The secondary outcomes were muscle histomorphology and histomorphometry as well as limb functional recovery. Muscle histomorphology was assessed using a semi-quantitative scoring of H & E stained slides at three different locations under light microscopy at 100x magnification. This scoring system assesses muscle fibers morphology and integrity, extracellular inflammatory infiltration (endomysial and perimysial), interstitial dilatation (endomysial and perimysial) and fibrosis (20). All items were scored using a 3-point scale, with 0 indicating absence of damage, 1: moderate damage, and 2: severe damage (**table IS**). Histomorphometric measures using image J included muscle fibers width and fibrocytes number count measured in six fields at 100x magnification. Muscle fibe width (µm) was assessed using the straight-line tool of image J, which measures the maximum distance between two opposing points of muscle fiber while fibrocytes count was calculated using analyze particles tool of image J. The worst score in each outcome measure (per animal specimen) was taken for comparison to determine the strain injury healing potentials.

Statistics

Descriptive statistics are presented as median and range. Due to the small sample size and non- normal distribution of the data, the non-parametric Kruskal and Wallis test was used followed by Mann-Whitney test to compare between groups. All statistical analyses were performed using the SPSS 21.0 for windows (IBM incorporation, IL, USA), with the p-value set at $p < 0.05$ to declare significance

RESULTS

One animal from the subacute injury group died spontaneously, leaving 31 animals for SFI scoring. For the remaining animals, a total of 29 specimens were assessed for histopathology and/or histomorphometry (two specimens were damaged during histological processing: one in normal and one in chronic injury groups).

Fascia histomorphometry (see table I, figures 1, 2)

Fascia thickness (µm) median (range) in the normal group was 190.3 (129.5-209.4) µm. The acute injury group showed the thickest fascia with a median (range) of 376.8 (130.8-908.1) µm. Compared to normal group, all injury groups had significantly thicker fascia ($p < 0.05$) **figure 2S**).

Collagen area (%) median (range) of the normal control group was 64.6 (51.1-76.4)%. The subacute injury group had the smallest area (%), with a median (range) of 50.7 (35.1-58.0)%. Collagen IntDen median (range) in the normal group was 690693.4 (545888.7- 815884.6). The subacute injury group showed the lowest IntDen: 542229.9 (374943.3- 619834.7). Both variables were significantly lower in the subacute injury group compared to normal and chronic injury groups ($p < 0.05$) (**figures 3S, 4S**).

Fibrocytes area (%) median (range) of the normal control group was 1.0 (1.0-2.5)%. The acute injury group showed the greatest increase of 4.3 (1.1- 6.9) % (**figure 5S**). Nucleus perimeter (µm) median (range) in the normal group was 34.1 (20.3-61.3) µm whereas the acute injury group had the largest perimeter of 68.3 (45.3-193.0) µm (**figure 6S**). The inflammatory area (%) median (range) of the normal control group was 0.5 (0.0-0.9) %. The acute injury group showed the greatest increase with a median of 2.4 (0.5- 4.2) % (**figure 7S**). Only the acute injury group showed significant increase of all cellular variables compared to the remaining groups ($p < 0.05$). The chronic injury group showed significant increase in inflamm - tory area (%) compared to normal group ($p = 0.045$), with only 28.50 % of this group rats showing signs of inflammation

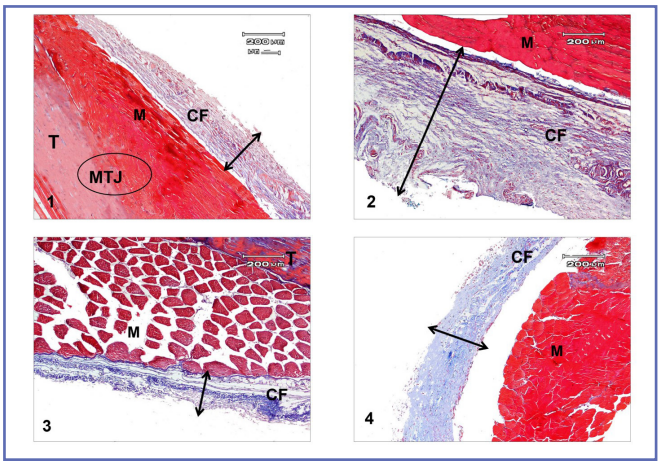

Figure 1. Photomicrograph of Masson stained histologic specimens of distal TA muscle (M) with the overlying crural fascia (CF) at 100X magnification.

1) Normal fascia thickness (2 headed arrows) with collagen fibers aligned parallel to each other within the same layer; 2) Acute injured rat with increased fascia thickness; 3) Subacute injured rat with decreased collagen area and density; and 4) Chronic injured rat with increased fascia thickness and collagen regained its density relative to the subacute stage. T: Tendon; MTJ: Myotendinous Junction.

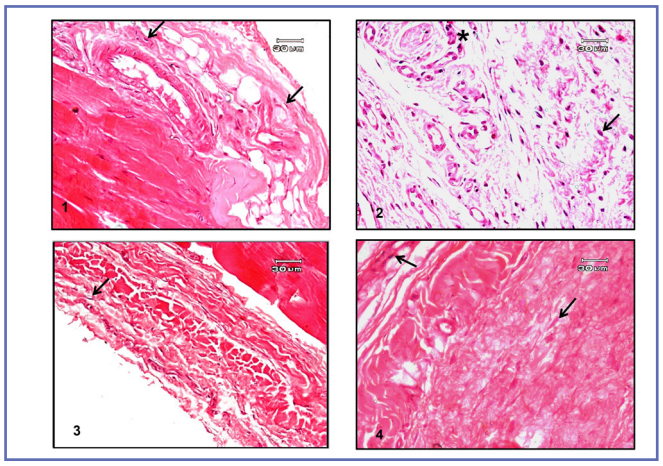

Figure 2. Photomicrograph of H & E stained histologic specimens of distal crural fascia (CF) at 400X magnification.

1) Normal rat with elongated fibrocytes (arrow); 2) Acute injured rat showing increased number of fibrocytes and enlarged nuclei with presence of inflammatory cells (Asterix); 3) subacute and 4) chronic injured rats with fibrocytes regaining their normal number and size with disappearance of inflammatory cells

Table I. Between groups comparisons of fascia histomorphometry.

	Normal	Acute	Sub-acute	Chronic
Fascia thickness (µm)	190.3 (129.5-209.4)	376.8 (130.8-908.1)	316.5 (145.3-510.0)	319.5 (155.2-595.7)
		p = **0.011**$^{a*(0.6)}$, 0.563$^{b(0.1)}$, 0.418$^{c(0.2)}$	p = **0.048**$^{a*(0.5)}$, 0.749$^{c(0.1)}$	p = **0.018**$^{a*(0.6)}$
Collagen area %	64.6 (51.1-76.4)	56.3 (39.3-69.3)	50.7 (35.1-58.0)	69.5 (45.7- 90.6)
		p = 0.105$^{a(0.4)}$, 0.130$^{b(0.4)}$, 0.105$^{c(0.4)}$	p = **0.009**$^{a*(0.7)}$, **0.034**$^{c*(0.6)}$	p = 0.565$^{a(0.1)}$

	Normal	Acute	Sub-acute	Chronic
Collagen integrated density	690693.4 (545888.7-815884.6)	6016561.8 (420280.9-740827.6)	542229.9 (374943.3 -619834.7)	742665.0 (488714.6 -968178.0)
		p = 0.105$^{a(0.4)}$, 0.164$^{b(0.4)}$, 0.105$^{c(0.4)}$	p = **0.009a*(0.7), 0.034c*(0.6)**	p = 0.565$^{a(0.1)}$
Fibrocytes area %	1.0 (1.0-2.5)	4.3 (1.1-6.9)	1.6 (0.4-2.5)	1.1 (0.8-2.1)
		p = **0.004**$^{a*(0.7)}$, **0.011b**$^{*(0.6)}$, **0.005**$^{c*(0.7)}$	p = 0.365$^{a(0.2)}$, 0.223$^{c(0.3)}$	p = 1.000$^{a(0.0)}$
Nucleus perimeter (µm)	34.1 (20.3-61.3)	68.3 (45.3-193.0)	36.3 (27.3- 59.2)	41.1 (22.5- 81.3)
		p = **0.005**$^{a*(0.7)}$, **0.003b**$^{*(0.8)}$, **0.021**$^{c*(0.6)}$	p = 0.749$^{a(0.1)}$, 0.848$^{c(0.1)}$	p = 0.565$^{a(0.1)}$
Inflammatory area%	0.5 (0.0-0.9)	2.4 (0.5- 4.2)	0.00 (0.0-1.5)	0.0 (0.0-0.8)
		p = **0.005**$^{a*(0.7)}$, **0.007b**$^{*(0.7)}$, **0.001**$^{c*(0.8)}$	p = 0.556$^{a(0.2)}$, 0.413$^{c(0.2)}$	p = **0.045**$^{a*(0.5)}$

Data are expressed as median, (min-max), p and effect size (R) values of the comparisons. *Significant level set at $p < 0.05$. [a]Compared to normal control group; [b]Compared to subacute injury group; [c]Compared to chronic injury group. $P^{(R)}$: R is the effect size.

Muscle histopathology and histomorphometry (see table II, figure 3)

Muscle fiber morphology and integrity scores for the normal animal's median (range) were 0 (0-1). The acute and subacute injury groups had the highest scores: 1 (1-2) and 1 (1), respectively (**figures 8S, 9S**). For histomorphometry, fibers width (µm) median (range) for the normal animals was 32.5 (21.5- 52.9) µm. The acute injury group had the highest score: 57.8 (34.9-68.0) µm (**figure 10S**). All muscle fibers parameters were significantly higher in the acute and subacute injury groups compared to the normal and chronic injury animal groups ($p < 0.05$).

For extracellular inflammatory infiltration, the endomysial and perimysial inflammatory scores median (range) for the normal animals were 0 (0-2). The acute injury group showed the highest percentage of rats showing signs of severe inflammation scoring 2 (1-2). The endomysial infla - matory score was significantly higher only in the acute injury group compared to normal and chronic injury groups and in the subacute injury group compared to chronic injury group ($p < 0.05$), whereas the perimysial inflammatory score was significantly higher only in this group compared to all remaining animal groups ($p < 0.05$) (**figures 11S, 12S**).

For interstitial dilatation, the endomysial and perimysial dilatation median (range) scores for the normal animals were 0

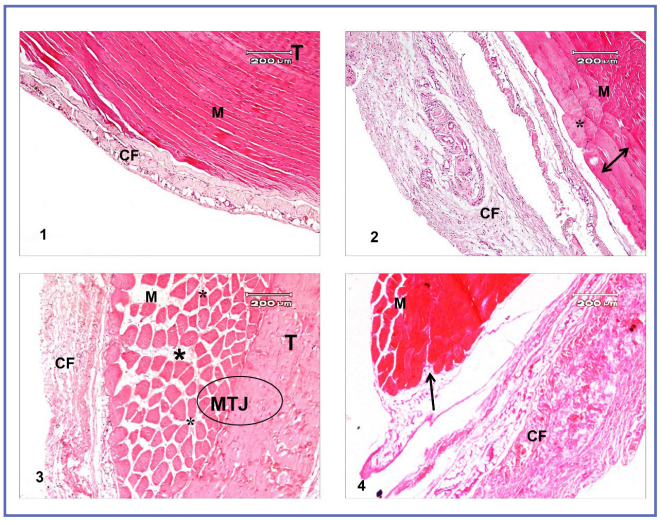

Figure 3. Photomicrograph of H & E stained histologic specimens of distal TA muscle (M) with the overlying crural fascia (CF) at 100X magnification.

1) Normal specimen with homogenous muscle fibers and minimal spacing between them; 2) Acute injured rat specimen with increased muscle fiber width (2 headed arrow) and endomysial inflammation (*); 3) Subacute injured rat specimen with heterogeneous muscle fibers and increased perimysial dilataion (*); 4) Chronic injured rat with homogenous muscle fiber but remaining fibrous tissue (1 headed arrow). T: Tendon; MTJ: Myotendinous Junction.

Table II. Between groups comparison of muscle histopathology and histomorphometry measures.

	Normal	Acute	sub-acute	Chronic
Muscle fibers morphology	0 (0-1)	1 (1-2)	1 (1)	0 (0-1)
		p = **0.004**$^{a*(0.7)}$, 0.080$^{b(0.5)}$, **0.009**$^{c*(0.7)}$	p = **0.007**$^{a*(0.7)}$, **0.023**$^{c*(0.6)}$	p = 0.591$^{a(0.1)}$
Fiber integrity	0 (0-1)	1 (1-2)	1 (1)	0 (0-1)
		p = **0.004**$^{a*(0.7)}$, 0.080$^{b(0.4)}$, **0.009**$^{c*(0.6)}$	p = **0.007**$^{a*(0.7)}$, **0.023**$^{c*(0.6)}$	p = 0.591$^{a(0.1)}$
Endomysial inflammatory infiltration	0 (0-2)	2 (1-2)	1 (0-2)	0 (0-1)
		p = **0.006**$^{a*(0.7)}$, 0.054$^{b(0.5)}$, **0.001**$^{c*(0.9)}$	p = 0.165$^{a(0.4)}$, **0.031**$^{c*(0.6)}$	p = 0.476$^{a(0.2)}$
Perimysial inflammatory infiltration	0 (0-2)	2 (1-2)	1 (0-1)	0 (0-1)
		p = **0.006**$^{a*(0.7)}$, **0.003**$^{b*(0.8)}$, **0.001**$^{c*(0.8)}$	p = 0.467$^{a(0.2)}$, 0.298$^{c(0.3)}$	p = 0.872$^{a(0.1)}$
Endomysial dilatation	0 (0-1)	1 (0-2)	2 (0-2)	0 (0-1)
		p = **0.022**$^{a*(0.6)}$, 0.667$^{b(0.1)}$, **0.007**$^{c*(0.7)}$	p = 0.114$^{a(0.4)}$, 0.059$^{c(0.5)}$	p = 0.530$^{a(0.2)}$
Perimysial dilatation	0 (0-1)	1.5 (0-2)	2 (0-2)	1 (0-1)
		p = **0.012**$^{a*(0.6)}$, 0.847$^{b(0.1)}$, **0.012**$^{c*(0.6)}$	p = **0.014**$^{a*(0.2)}$, **0.014**$^{c*(0.7)}$	p = 1.000$^{a(0.0)}$
Fibrosis	0 (0-1)	0 (0-2)	1 (1)	1 (1)
		p = 0.533$^{a(0.2)}$, 0.178$^{b(0.3)}$, 0.178$^{c(0.3)}$	p = **0.007**$^{a*(0.7)}$, 1.000$^{c(0.0)}$	p = **0.007**$^{a*(0.7)}$
Fiber width (µm)	32.5 (21.5-52.9)	57.8 (34.9-68.0)	46.5 (37.2-93.6)	35.5 (28.5- 49.3)
		p = **0.025**$^{a*(0.6)}$, 0.655$^{b(0.1)}$, **0.025**$^{c*(0.6)}$	p = **0.025**$^{a*(0.6)}$, **0.025**$^{c*(0.6)}$	p = 0.654$^{a(0.2)}$
Cellularity number	148 (65- 202)	288 (166-336)	128 (80- 150)	180 (21- 196)
		p = **0.004**$^{a*(0.8)}$, **0.002**$^{b*(0.8)}$, **0.013**$^{c*(0.7)}$	p = 0.306$^{a(0.3)}$, 0.096$^{c(0.4)}$	p = 0.482$^{a(0.2)}$

Data are represented as median, (min- max), p and effect size (R) values of the comparisons. *Significant level set at $p < 0.05$. [a]Compared to normal control group; [b]Compared to subacute injury group; [c]Compared to chronic injury group. $P^{(R)}$: R is the effect size.

(0-1). The subacute injury group showed the highest percentage of rats having the greatest dilatation: 2 (0-2). The endomysial dilatation score was significantly higher only in the acute injury group compared to normal and chronic injury groups ($p < 0.05$), whereas perimysial dilatation was significantly higher in acute and subacute injury groups compared to normal and chronic injury groups ($p < 0.05$) (**figures 13S, 14S**).

Morphometric fibrocytes number median (range) for the normal animals was 148 (65- 202). The acute injury group had the highest fibrocyte number: 288 (166-336). Only the acute injury group significantly had greater cell count compared to the remaining animal groups ($p < 0.05$) (**figure 15S**).

Fibrosis median (range) score for the normal animals group was 0 (0-1). Only the subacute and chronic injury groups showed the greatest amount of fibrosis with all animals scored as one, which was significantly higher than the normal group ($p < 0.05$) (**figure 16S**).

SFI results

The SFI median (range) scores were: - 14.8 (- 18.3-1.9) for the normal control, - 13.9 (- 29.1 - - 3.8) for the acute, - 14.7 (- 36.4 - - 0.1) for the subacute, and - 12.4 (- 29.3-1.8) for the chronic injury groups. All groups were not statistically different ($p > 0.05$) (**figure 17S**).

DISCUSSION

This study describes the histomorphological and histopathological changes in fascia and muscle as well as lower limb function during muscle strain injury healing from the acute through the chronic stages. Studying strain injury in humans is challenged by random onset and variable clinical presentations of injury. Thus, animal models are optimal in controlling such confounders allowing controlled investigation of injury mechanisms and their associated changes *in vivo*. In this study, muscle strain was induced by passive elongation of the TA muscle using a simple, valid and reliable method (14). The current study provides evidence that fascia and muscle pathological changes almost fully recover spontaneously by the chronic stage. On the other hand, there was no evidence of limb functional impairment at any given stage.

In this study, strain was induced in TA muscle as it has easily accessible superficial parallel muscle fibers, which allows applied force to act uniformally on muscle fibers and the MTJ (21). Previous studies focused on investigating eccentric strain rather than strain secondary to passive stretch, thus, we opt to compare the current study results to what is available in literatures regardless to the method of strain induction. Strain injury is associated with acute inflammatory response that is characterized by fibrocytes proliferation and inflammator infiltration starting from the 1st hour after injury and lasting up to 7 days (22). This is in an agreement with the findings of the current study that fibrocytes and inflammatory cells number increased in both fascia and muscle tissues in the acute stage and returned to normal values by the subacute stage. This inflammatory response may have an important role in clearing tissue debris and stimulating the regenerative property of muscle stem cells in order to facilitate regeneration (23). Only two rats (28.5%) in the chronic group showed persistent fascia inflammation. This could be attributed to individual animal responses to strain injury. Furthermore, evidence supports that mononuclear cells can reside in normal tissue and can be stimulated by different pathophysiological situations (24).

Muscle and fascia showed collagen and sarcoplasmic membrane degeneration. These changes were evident earlier in muscle (acute stage) than in fascia (subacute stage). Early appearance of muscle changes, prior to fascia, could be explained by MTJ being the primary site of induced injury (13). MTJ is a transitional zone between muscle fibers and tendon. It is a site rich in collagen contents especially collagen XXII which is not evident elsewhere in muscle and tendon and might contribute to MTJ stiffness and reduced energy absorption capacity compared to its surrounding structures (25). The reduction in collagen in the current findings is in an agreement with the previous observation that fibers damage following eccentric strain precedes phagocytosis at the injury site (26). Also, this damage may have continued through the subacute stage, whereas signs of regeneration appeared approximately at the chronic stage. This has been previously reported after active eccentric muscle strain in humans (27). In the current study, collagen structure recovery in muscle and fascial tissues was apparent by the chronic stage. This recovery could be expected as this model shows mild induced strain which previously showed full reversibility of collagen linking when tested mechanically *in vitro* (28).

Fascia thickness, muscle fibers width, and interstitial tissue spaces increased in the acute and subacute stages. The increase shown in the acute stage could partly be attributed to tissue swelling associated with the early inflammat - ry response, which usually resolves by the 7th day (7). On the other hand, tissue repair and remodeling are thought to start by the end of the 1st week and peaks by the 2nd (29). The increased structural volume associated with this process might be responsible for the persistent geometric increase in tissue size. Increased muscle fibers width during the subacute stage was associated with an evident fibrous healing, considering that the MTJ is the main site of strain injury (13). By the chronic stage, fascia thickness increased, which might be a consequence of random collagen laydown prior to completion of tissue remodeling, a process that is expected to take longer time than that occurring in muscle tissue as

was shown in eccentric-induced strain injuries (30). On the other hand, although muscle restored normal fibers width, yet fibrotic tissue continued to be evident (31). Scar tissue usually matures around the 2nd week and continues afterwards (7, 13). This reparative process could be expected to negatively influence muscle mechanics and full regeneration. Structural changes were not only confined to the crural fascia and TA muscle, but also to all examined intramuscular CTs. At the acute stage, endo and perimysial spaces showed obvious increased dilatation and inflammatory infiltration. Endomysium may play a substantial protective role for muscle against strain. This is in line with the predictions based on biomechanical modeling that endomysium may play a substantial role in providing passive resistance to excessive overstretch and strains within fibers at the MTJ (32). The observed extracellular matrix (ECM) inflammation is in an agreement with similar findings associated with active eccentric strain in humans where greater inflammation was observed in the perimysium than the endomysium (33). By the subacute stage, fibrosis started to appear in the perimysium, a change that continued throughout the chronic stage. Inflammatory cells release growth factors that trigger fibroblasts to synthesize collagen and fibrosis within the ECM. Reduced matrix flexibility may result in muscle shortening, limited extensibility, and increased risk of recurrence. The current study showed no evidence to support changes in limb function as measured by SFI during various healing stages following strain injury. This is in an agreement with the findings of Ramos *et al.* (14) who reported deterioration of SFI scores that was evident by 12 h only and recovered after 24 h. As animals were allowed free cage mobility, thus, animals practiced the usual functional tasks that were similar to that assessed by the SFI testing, an activity which may have preserved their normal locomotion pattern. Normal performance in SFI testing doesn't guarantee optimal performance in sports field as the latter put more stresses on the musculoskeletal system. In the future, rats can be assessed using more challenging tests than SFI to give a more relevant clinical picture of how they would perform in sport activities.

Identifying that fascial injury is a part of the strain injury and how it heals through the different stages and targeting them in treatment would likely to affect the rehabilitation outcomes. Recurrence of strain injury in sports is a common problem that can occur during rehabilitation or early after athletes return to sport (34) as was proved in hamstrings reinjury that occurred at the same location with a more severe nature (35). Recurrence can be referred to incomplete tissue healing or injured tissues that were not previously considered to be affected by the strain injury. Even more it has been found that the amount of ECM injury affects the prognosis and recurrence (36).

There are general guidelines concerning treatments that can be applied in different healing stages of strain injury (37) but their effects are not known for the fascial injured tissues. For example, it was suggested that short period of immobilization followed by mobilization after strain injury is the best for collagen, but their effects were tested on muscular tissue only (38) and is not known if certain types of loading early after strain injury would favor fascia healing. Based on our results, we recommend investigating the effect of manual therapies such as friction massage or loading exercises at the subacute and chronic stages as scar tissue and collagen malalignment seems to be the persistent pathological changes in fascial injured tissues. Further, fascia healing in humans may be investigated using imaging techniques such as US and MRI and to correlate the effect of adding fascia therapy to strain injury healing and the rate of injury recurrence. To authors' knowledge, this is the first longitudinal study to describe fascia and muscle changes associated with stretch-induced passive muscle strain in different healing stages using quantitative objective and semi-quantitative methods. In this study, potential risks of bias were minimized by employing assessor's training and blindness as well animals' grouping and specimens' randomization and concealment. However, a few limitations exist: first, the nature of animal research and the destructive nature of the histopathological outcome measures made it impossible to have baseline data for the same rats. As animals are generally homogenous, the control data were assumed to reflect baseline values. Second, although in this study animals were followed until the chronic stage, yet studies are recommended to consider a longer follow-up period until full recovery is accomplished. Third, only structural changes and limb kinematics are reported. Future studies are encouraged to assess tissue mechanics, which is an important determinant for full tissue recovery. Also, future studies may consider measuring other variables that may reflect tissue stiffness such as changes in the core temperature or using ultrasound elastography. Further, studying changes at the molecular level and the use of *in vivo* imaging techniques may give clearer insights into strain-associated changes at different intervals for the same rats.

CONCLUSIONS

In summary, this study provides evidence that fascia and muscle structural changes are apparent by the acute stage and almost recover by the chronic stage. In the acute stage, both muscle and fascia structures showed hypercellularity and inflammatory infiltration. In the subacute stage, the two tissues showed significant collagen degradation. By the chronic stage, increased fascia thickness and muscle fibrosis were the only remaining residuals. Future studies are recommended to investigate therapeutic interventions that may address fascia in rehabilitation in order to optimize full tissue recovery.

PREVIOUS PUBLICATION

An abstract based on preliminary findings of this study have been orally presented at the 1st virtual congress of the European Federation of Orthopedic and traumatology (EFFORT) that was held online from October 28-30, 2020 (Abstract #1853).

FUNDINGS

This study was partially funded by Cairo University.

DATA AVAILABILITY

Data are available under reasonable request to the corresponding author.

CONTRIBUTIONS

NAE: conceptualization, experiment refining, planning and conduction, data analysis and interpretation, manuscript writing and revision. TM, HW, MM, MN: experimental part partecipation and final manuscript approval. NSH: histological scoring supervision and partecipation, image capturing and final manuscript approval. ARY: conceptualization, experiment refining and designing, study supervision conduction, data analysis revision, results interpretation, and final manuscript revision and approval

CONFLICT OF INTERESTS

The authors declare that they have no conflict of interests.

REFERENCES

1. Huijing PA, Yaman A, Ozturk C, Yucesoy CA. Effects of knee joint angle on global and local strains within human triceps surae muscle: MRI analysis indicating in vivo myofascial force transmission between synergistic muscles. Surg Radiol Anat 2011;33(10):869-79.
2. Purslow PP. The Structure and Role of Intramuscular Connective Tissue in Muscle Function. Front Physiol 2020;11:495.
3. Wilke J, Vleeming A, Wearing S. Overuse Injury: The Result of Pathologically Altered Myofascial Force Transmission? Exerc Sport Sci Rev 2019;47(4):230-6.
4. Garrett WE. Muscle strain injuries: Clinical and basic aspects. Med Sci Sports Exerc 1990;22(4):436-43.
5. Verrall G, Dolman B. Deducing a mechanism of all musculoskeletal injuries. Muscles Ligaments Tendons J 2016 17;6(2):174-82.
6. Chan O, Del Buono A, Best TM, Maffulli N. Acute muscle strain injuries: a proposed new classification system. Knee Surg Sports Traumatol Arthrosc 2012;20(11):2356-62.
7. Nikolaou PK, Macdonald BL, Glisson RR, Seaber AV, Garrett WE Jr. Biomechanical and histological evaluation of muscle after controlled strain injury. Am J Sports Med 1987;15(1):9-14.
8. Mohammad T, Youssef AR. Time to recovery of sciatic function index after induced tibialis anterior strain in rats. Muscles Ligaments Tendons J 2017;7(3):576–82.
9. Jakobsen JR, Jakobsen NR, Mackey AL, Koch M, Kjaer M, Krogsgaard MR. Remodeling of muscle fibers approaching the human myotendinous junction. Scand J Med Sci Sports 2018;28(8):1859-65.
10. Prakash A, Entwisle T, Schneider M, Brukner P, Connell D. Connective tissue injury in calf muscle tears and return to play: MRI correlation. Br J Sports Med 2018;52(14):929–33.
11. Wilke J, Hespanhol L, Behrens M. Is It All About the Fascia? A Systematic Review and Meta-analysis of the Prevalence of Extramuscular Connective Tissue Lesions in Muscle Strain Injury. Orthop J Sports Med 2019;7(12):2325967119888500.
12. An YH, Freidman RJ. Animal Models in Orthopaedic Research. Animal Models in Orthopaedic Research. Boca Raton: CRC Press, 1998.
13. Järvinen TA, Kääriäinen M, Järvinen M, Kalimo H. Muscle strain injuries. Curr Opin Rheumatol 2000;12(2):155-61.
14. Ramos L, Leal Junior EC, Pallotta RC, *et al*. Infrared (810 nm) low-level laser therapy in experimental model of strain-induced skeletal muscle injury in rats: effects on functional outcomes. Photochem Photobiol 2012;88(1):154-60.
15. de Medinaceli L, Freed WJ, Wyatt RJ. An index of the functional condition of rat sciatic nerve based on measurements made from walking tracks. Exp Neurol 1982;77(3):634-43.
16. Guzmán-Valdivia CH, Blanco-Ortega A, Oliver-Salazar MA, Carrera-Escobedo JL. Therapeutic Motion Analysis of Lower Limbs Using Kinovea. Int J Soft Comput Eng 2013;3(2):359–65.
17. Bain JR, Mackinnon SE, Hunter DA. Functional evaluation of complete sciatic, peroneal, and posterior tibial nerve lesions in the rat. Plast Reconstr Surg 1989;83(1):129-38.
18. Morales-Avalos R, Soto-Domínguez A, García-Juárez J, *et al*. Morphological and histomorphometric evaluation of the ventral rectus sheath of the rectus abdominis muscle, fascia lata and pectoral fascia. The beginning of a morphological information bank of human fascias. Histol Histopathol 2017;32(3):271-82.
19. Montanholi YR, Haas LS, Swanson KC, Coomber BL, Yamashiro S, Miller SP. Liver morphometrics and metabolic blood profile across divergent phenotypes for feed efficie - cy in the bovine. Acta Vet Scand 2017;59(1):24.
20. Rizo-Roca D, Ríos-Kristjánsson JG, Núñez-Espinosa C, *et al*. A semiquantitative scoring tool to evaluate eccentric exercise-induced muscle damage in trained rats. Eur J Histochem 2015;59(4):2544.
21. Raiteri BJ, Cresswell AG, Lichtwark GA. Muscle-tendon length and force affect human tibialis anterior central aponeurosis stiffness in vivo. Proc Natl Acad Sci U S A 2018;115(14):E3097-E3105.

22. Raastad T, Risoy BA, Benestad HB, Fjeld JG, Hallen J. Temporal relation between leukocyte accumulation in muscles and halted recovery 10-20 h after strength exercise. J Appl Physiol (1985) 2003;95(6):2503-9.
23. Toumi H, F'guyer S, Best TM. The role of neutrophils in injury and repair following muscle stretch. J Anat 2006;208(4):459-70.
24. Pillon NJ, Bilan PJ, Fink LN, Klip A. Cross-talk between skeletal muscle and immune cells: muscle-derived mediators and metabolic implications. Am J Physiol Endocrinol Metab 2013;304(5):E453-65.
25. Koch M, Schulze J, Hansen U, *et al*. A novel marker of tissue junctions, collagen XXII. J Biol Chem 2004;279(21):22514-21.
26. Suzme R, Yalcin O, Gurdol F, Gungor F, Bilir A. Connective tissue alterations in women with pelvic organ prolapse and urinary incontinence. Acta Obstet Gynecol Scand 2007;86(7):882-8.
27. Jones DA, Newham DJ, Round JM, Tolfree SE. Experimental human muscle damage: morphological changes in relation to other indices of damage. J Physiol 1986;375:435-48.
28. Vader D, Kabla A, Weitz D, Mahadevan L. Strain-induced alignment in collagen gels. PLoS One 2009;4(6):e5902.
29. Laumonier T, Menetrey J. Muscle injuries and strategies for improving their repair. J Exp Orthop 2016;3(1):3–15.
30. Mackey AL, Kjaer M. Connective tissue regeneration in skeletal muscle after eccentric contraction-induced injury. J Appl Physiol (1985) 2017;122(3):533-40.
31. Sikes KJ, Andrie KM, McConnell A, *et al*. Clinical and Histologic Manifestations of a Novel Rectus Femoris Myotendinous Junction Injury in Rats. Muscle Ligaments Tendons J 2021;11(04):600-13.
32. Stauber WT, Clarkson PM, Fritz VK, Evans WJ. Extracellular matrix disruption and pain after eccentric muscle action. J Appl Physiol 1990;69(3):868–74.
33. Huard J, Li Y, Fu FH. Muscle injuries and repair: current trends in research. J Bone Joint Surg Am 2002;84(5):822-32.
34. Green B, Lin M, McClelland JA, *et al*. Return to Play and Recurrence After Calf Muscle Strain Injuries in Elite Australian Football Players. Am J Sports Med 2020;48(13):3306-15.
35. Wangensteen A, Tol JL, Witvrouw E, *et al*. Hamstring Reinjuries Occur at the Same Location and Early After Return to Sport: A Descriptive Study of MRI-Confirmed Reinjuries. Am J Sports Med 2016;44(8):2112-21.
36. Balius R, Alomar X, Pedret C, *et al*. Role of the Extracellular Matrix in Muscle Injuries: Histoarchitectural Considerations for Muscle Injuries. Orthop J Sports Med 2018;6(9):2325967118795863.
37. Maffulli N, Oliva F, Frizziero A, *et al*. ISMuLT Guidelines for muscle injuries. Muscles Ligaments Tendons J 2013;3(4):241-9.
38. Järvinen MJ, Lehto MU. The effects of early mobilisation and immobilisation on the healing process following muscle injuries. Sports Med 1993;15(2):78-89.

SUPPLEMENTS

Table IS. Semiquantitative scoring tool to assess muscle damage adopted from Rizo-roca *et al*. (20).

Domain	0	1	2
Muscle fibers morphlology Abnormal (small, rounded, angular, splitted or hypertrophied fibers	< 4 fiber	4-7 fiber	> 7 fibers or entire fascicle
Muscle fibers integrity Necrotic or degenerating (basophilic, light stained, central nuclei or myophagocytosed fibers	absent	1-2 fiber	> 2 fiber
Endomysial inflammatory infiltration Small, mononuclear cells in the endomysium	< 6 cells	≥ 6 cells or 1 cluster	> 1 cluster or entire fascicle
Perimysial inflammatory infiltration Small, mononuclear cells in the perimysium	≤ 10 cells	> 10 cells	> 2 clusters or widely diffused
Endomysial dilatation Space between individual muscle fiber	Tight space	Moderately distended	completely distended
Perimysial dilatation Space between fasicles	Tight space	Moderately distended	completely distended

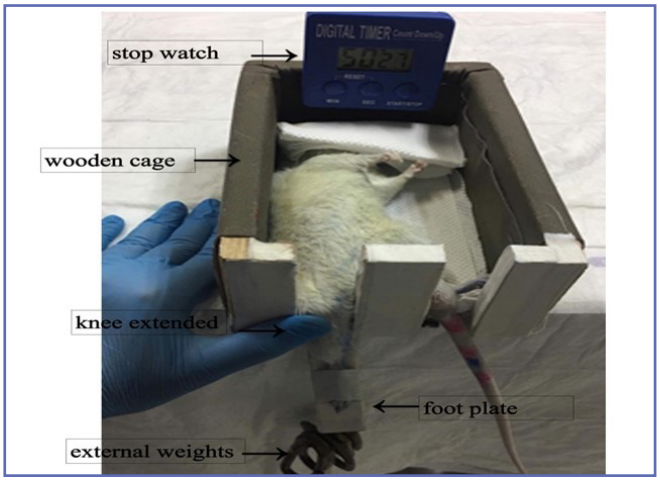

Figure 1S. Strain induction setup.

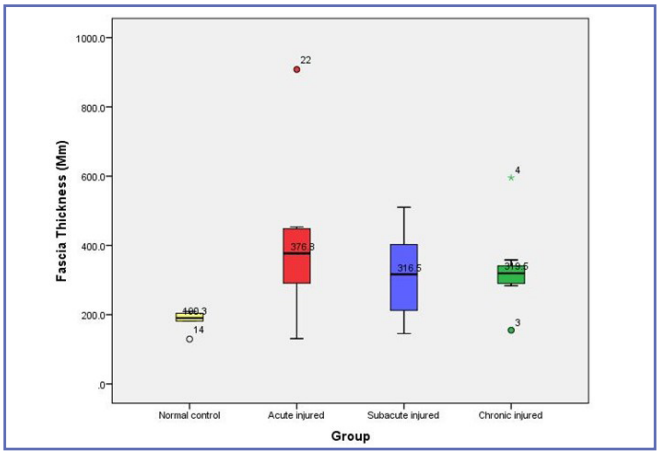

Figure 2S. Boxplots showing fascia thickness scores in all animal groups.

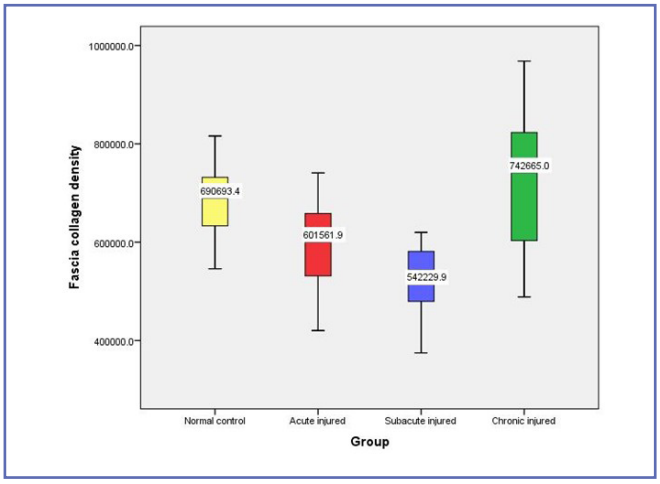

Figure 3S. Boxplots showing fascial collagen density in all animal groups

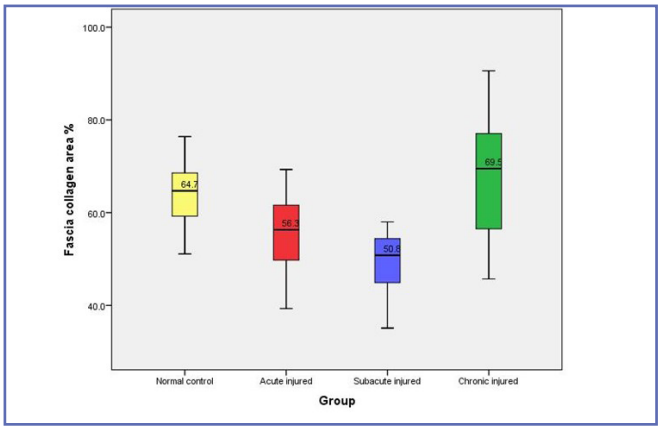

Figure 4S. Boxplots showing fascial collagen area (%) scores in all animal groups.

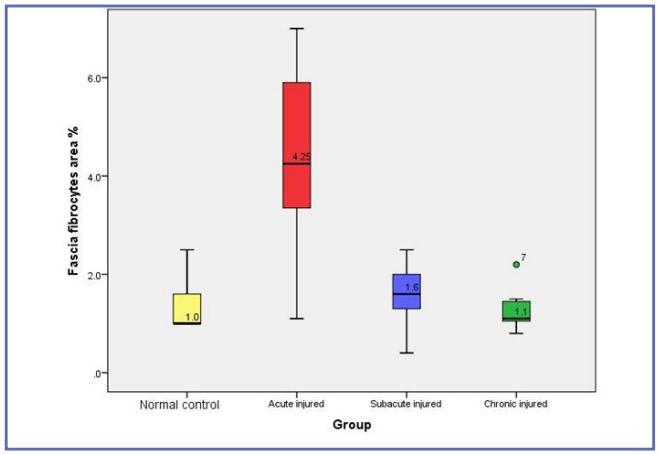

Figure 5S. Boxplots showing fascial fibrocytes area (%) scores in all animal groups.

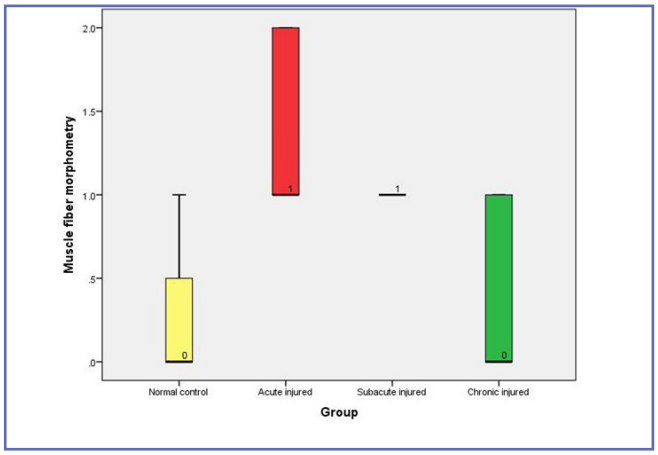

Figure 8S. Boxplots showing muscle fiber morphometry scores in all animal groups.

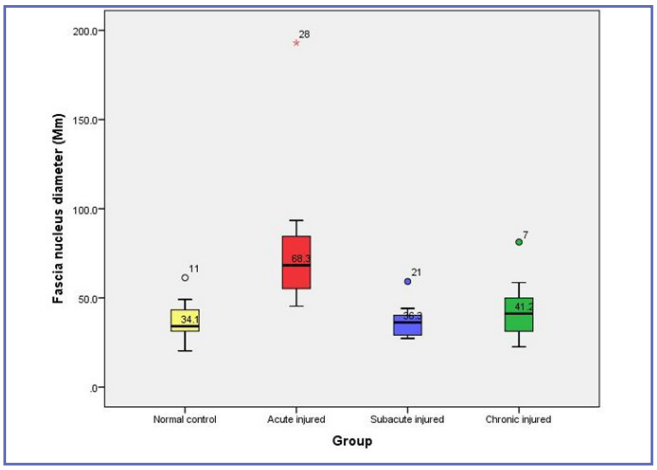

Figure 6S. Boxplots showing fascial nucleus perimeter scores in all animal groups.

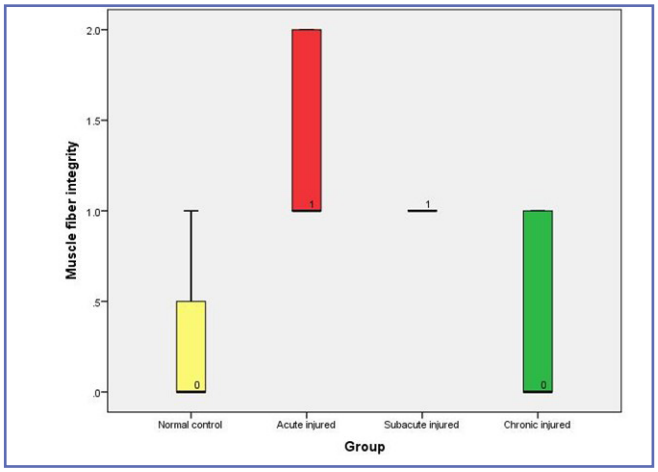

Figure 9S. Boxplots showing muscle fiber integrity scores in all animal groups.

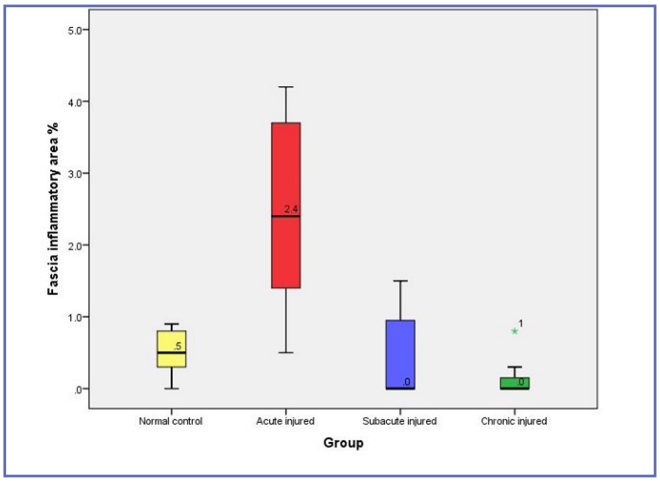

Figure 7S. Boxplots showing fascial inflammatory area (%) scores in all animal groups.

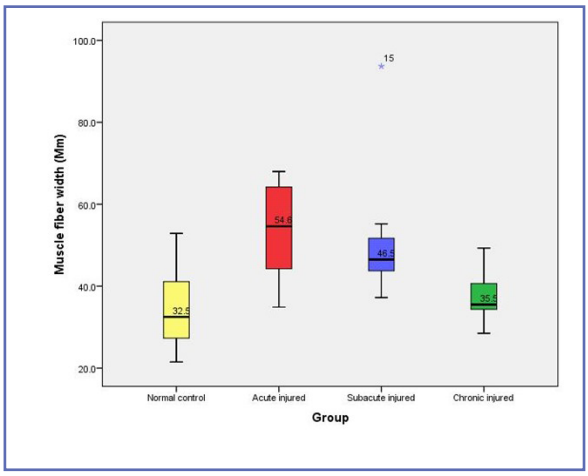

Figure 10S. Boxplots showing muscle fiber width scores in all animal groups.

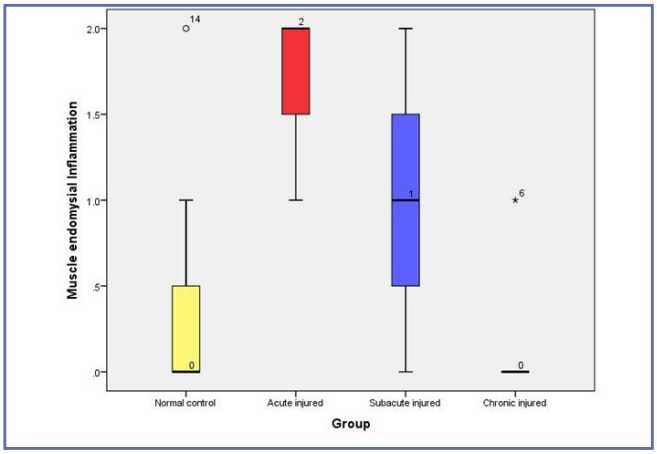

Figure 11S. Boxplots showing muscle endomysial inflammation scores in all animal groups.

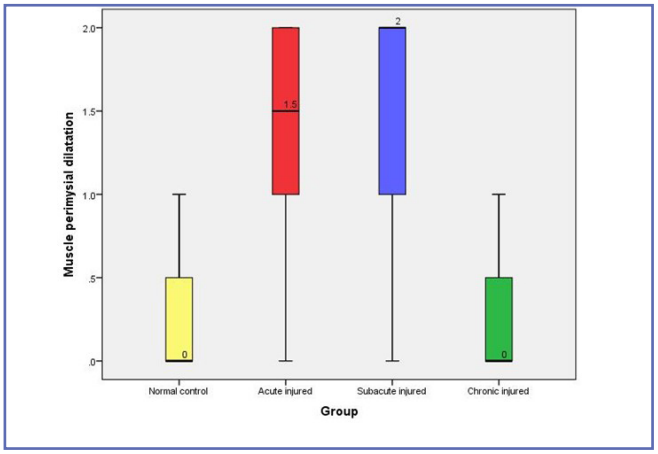

Figure 14S. Boxplots showing muscle perimysial dilatation scores in all animal groups.

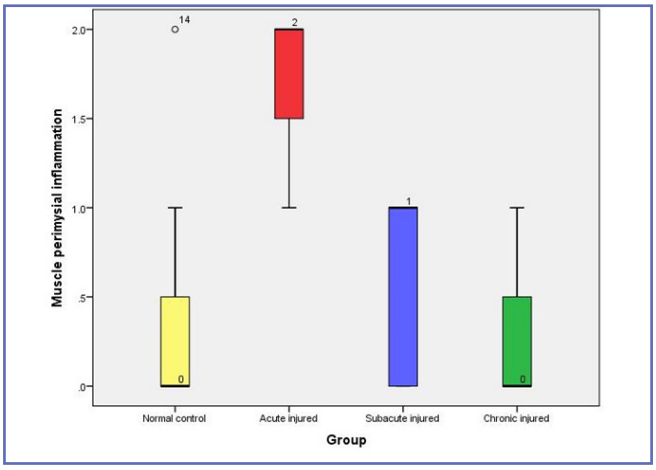

Figure 12S. Boxplots showing muscle perimysial inflammation scores in all animal groups.

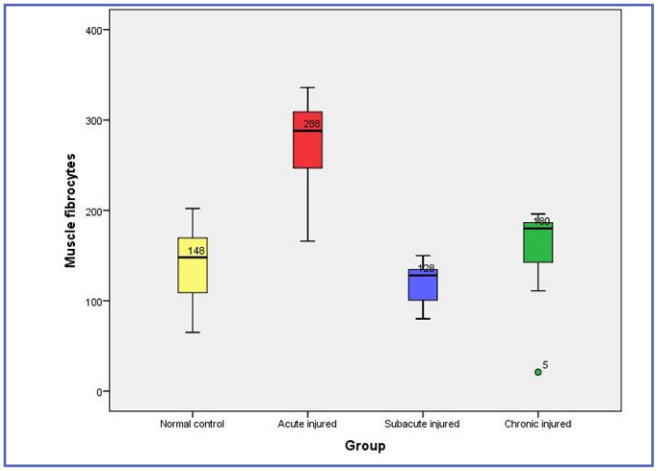

Figure 15S. Boxplots showing muscle fibrocytes scores in all animal groups.

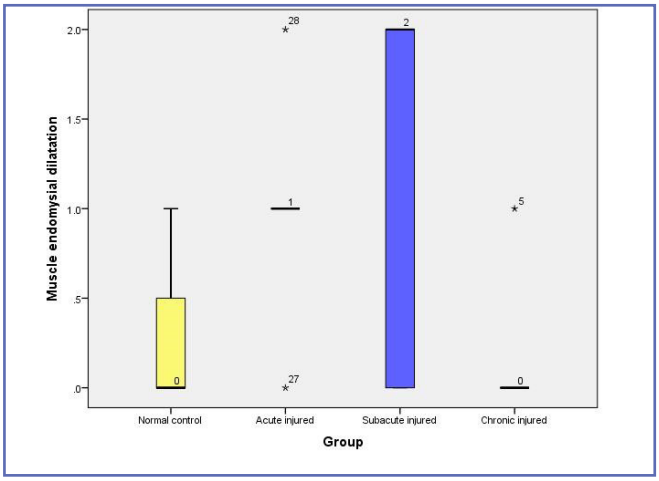

Figure 13S. Boxplots showing muscle endomysial dilatation scores in all animal groups.

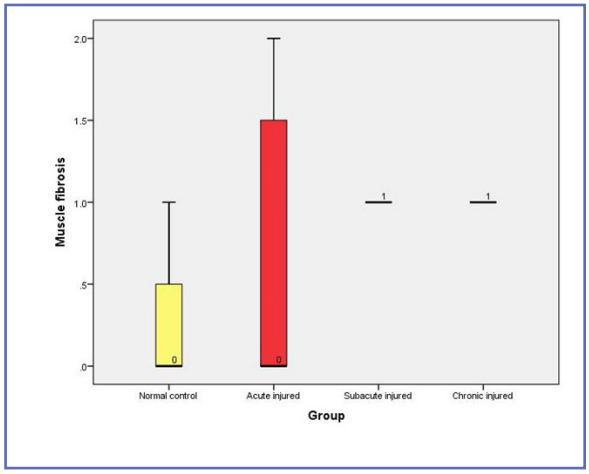

Figure 16S. Boxplots showing muscle fibrosis scores in all animal groups.

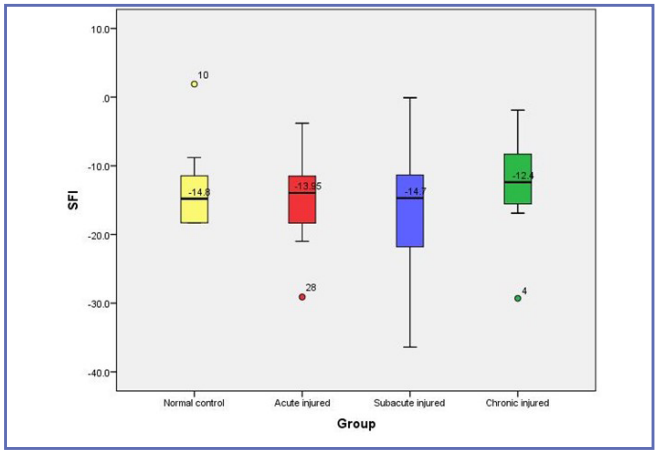

Figure 17S. Boxplots showing the SFI scores of all animal groups.

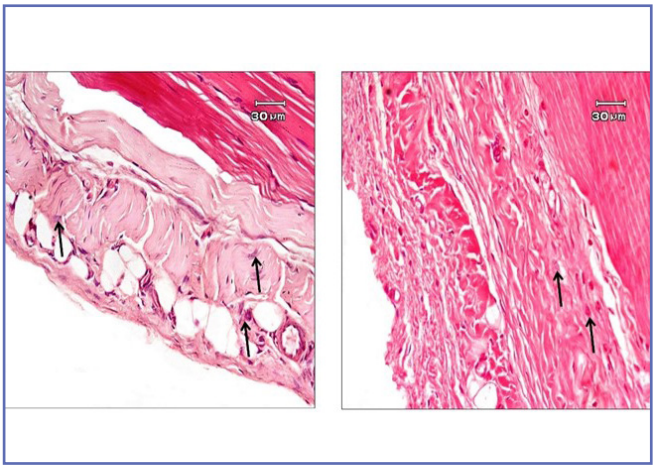

Figure 18S. Images for normal rats showing nuclei of fascial fibrocytes.

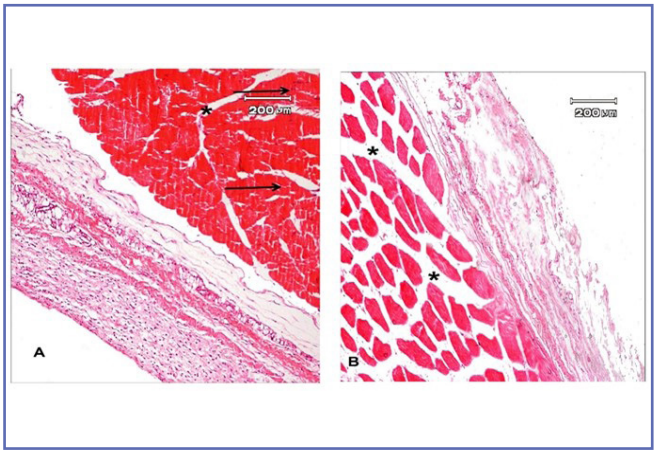

Figure 19S. Images for muscle in **(A)** acute and **(B)** subacute stages of strain injury.
Asterix (*) represent the perimysial dilatation and inflammation while arrows represent the endomysial inflammation and dilatation